UDC/UDK 539.42:669.24
Original scientific article/Izvirni znanstveni članek

ISSN 1580-2949
MTAEC9, 41(2)67(2007)

THERMAL FATIGUE OF A Ni-BASED SUPERALLOY SINGLE CRYSTAL

TERMIČNA UTRUJENOST MONOKRISTALA IZ NIKLJEVE SUPERZLITINE

[1]Leonid Getsov, [2]Natalia Dobina, [2]Alexandr Rybnikov

[1]Department of Strength of Materials, St. Petersburg State Politechnical University, St. Petersburg, Russia
[2] NPO ZKTI, Russia
guetsov@online.ru

Prejem rokopisa – received: 2006-07-01; sprejem za objavo – accepted for publication: 2006-11-29

This paper presents a thermal-mechanical fatigue (TMF) test procedure and some results obtained in vacuum for a Ni-based superalloy single crystal. This procedure allows the monitoring of slip lines, fatigue-crack initiation and propagation until final failure. Single-crystal specimens with different crystallographic orientations were tested under different thermal-cyclic loading conditions. Tests were conducted on smooth specimens as well as on specimens with a central hole of 0.5 mm diameter to analyze the effects of stress concentration. Both crystallographic and non-crystallographic cracks were observed. An increase of the maximum temperature in the cycle (with the same amplitude of temperature change) causes a severe shortening of the service life, as well as stress concentration. It was observed that the first initiated microcrack arrests and the sample fracture takes place on newly nascent microcracks.

Key words: thermal fatigue, single crystal, crystallographic orientation, crack, concentrator

V članku je opisana procedura za določitev termičnega utrujanja (TMF) in nekateri rezultati preizkusov monokristala iz nikljeve superzlitine v vakuumu. Procedura omogoča opazovanje drsnih črt ter začetek in propagacijo razpok do končnega preloma. Monokristali z različno prostorsko orientacijo so bili preizkušani pri različnih pogojih termično ciklične obremenitve. Preizkusi so bili izvršeni na gladkih preizkušancih in na takih s centralno izvrtino s premerom 0,5 mm zaradi analize koncentracije napetosti. Opažene so bile kristalografske in rekristalografske razpoke. Povišanje najvišje temperature v ciklu (pri enakem razponu spremembe temperature) povzroči veliko skrajšanje uporabne dobe, enak je vpliv koncentracije napetosti. Ugotovljeno je bilo, da se prva mikrorazpoka ustavi in da prelom nastane zaradi novo nastalih mikrorazpok.

Ključne besede: termična utrujenost, monokristal, kristalografska orientacija, razpoka, koncentrator

1 INTRODUCTION

Thermal-fatigue crack initiation in single-crystal aerofoils is the major cause of damage during turbine operation. A detailed study of fatigue-crack initiation and growth has been made [1-5]. This paper describes a new thermal-cyclic vacuum test procedure. During vacuum testing, this procedure makes it possible to monitor the crystallographic slip orientations, crack initiation and growth.

The publications [8-12] present a detailed review of research on the strength of single-crystal superalloys, carried out on the basis of an analysis of the literature with most of the attention paid to the publications of Russian researchers and, in particular, the authors of this paper. The problems of the influence of the anisotropy of single-crystal superalloys on the parameters of fatigue and the thermal-fatigue strengths are considered; some basic phenomenological and physical models of the material for the calculation of the deformation mode in single crystals are described and the criteria of thermal-fatigue fractures are discussed. Different aspects of the initiation and the evolution of the creep, fatigue and thermal fatigue cracks in single-crystal materials are considered, and their dependence on the temperature parameters, crystallographic orientation and their formation development mode was surveyed. Approaches to the definition of the fracture criteria and the methods of determining the deformation mode have been analyzed. Considerable attention is paid to the examination of the process of fatigue-crack development in single-crystals superalloys in the cases of HCF and LCF. The crystallographic peculiarities of fatigue failure and the criteria for the determination of the crack-growth direction and the rate at the different stages are considered. Special attention is paid to the conditions of the transition between stages.

2 EXPERIMENTAL PROCEDURE

2.1 Test procedure. A comprehensive procedure is developed in NPO CKTI for the determination of the thermal fatigue resistance of the various materials and coatings. A flat specimen is rigidly fixed in the vacuum chamber and cyclically heated with electric current (**Figure 1**). The heating is carried out according to the specified program (**Figure 2**) and automatically maintained during the testing. With the increase of the vacuum depth, the ultimate cycle temperature increases also. The temperature is measured with the rate of oxide-film formation on the sample surface. The slip

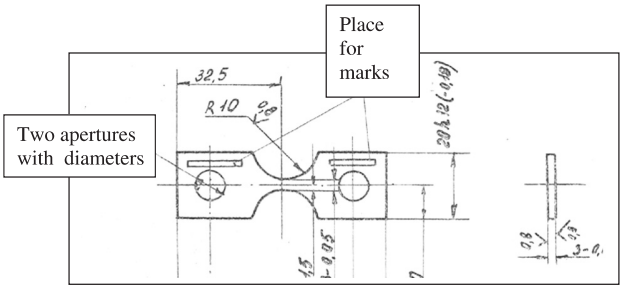

Figure 1: Specimen shape and size
Slika 1: Oblika in mere preizkušanca

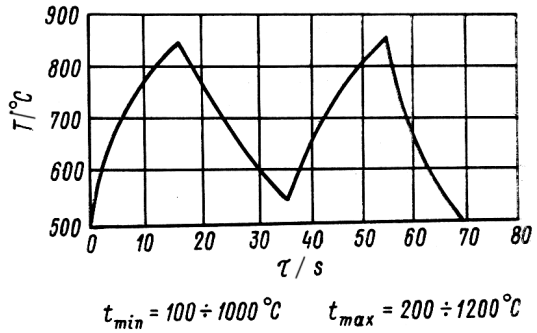

Figure 2: Program of the temperature-cycle variation
Slika 2: Program temperaturnega cikla

lines and surface microcracks are observed with an optical microscope [6].

The technique enables to:

- Determine the thermo-fatigue resistance for gas-turbine blades based on crack initiation and propagation.
- Compare of different material-processing techniques, parts manufacturing, repair and coating technologies by TMF resistance.
- Perform fatigue tests of small-scale specimens cut out from the gas-turbine blades after operation.
- To define the minimum thermal fatigue resistance of construction elements including composite materials, single-layer and multilayer coatings and welded joints.
- To study the details of the mechanism of thermal fatigue for material for various cycle parameters.
- To study the effect of stress concentration on the thermal fatigue.
- To determine crack orientations (ratio of $\Delta K_I/\Delta K_{II}$), the crack propagation rate, and the effect of the cycle's parameters on the crack propagation and on the thermal fatigue service life.

2.2 With testing the following parameters are determined: characteristic properties of the deformation relief defining the mechanism of thermal-fatigue damage accumulation; the number of cycles to the first appearance of the microcrack in the speciment and in the coating; the growth rate of incipient cracks and the number of cycles to sample failure.

The amplitude value of conventional elastic stresses is determined according to:

$$\Delta\sigma = (E_{st1}\alpha_1 T_{max} - E_{st2}\alpha_2 T_{min})\varphi$$
$$\varphi = 1 - \Delta k / \Delta l \quad (1)$$

where Δk is the measured value of the displacement during the cycle of control micro-hardness marks, applied on the sample surface along its working part edges; E_{st} is a static module of elasticity; and Δl is the free movement of the control marks during the heating from T_{min} to T_{max}.

The stress-strain relationship and the inelastic deformation evolution are calculated using a structural model [7]. The specific feature of this procedure and those of Coffin are the constant stresses over the sample's cross-section.

The number of cycles to failure of flat samples in vacuum and of tube samples in air that were tested using the different test units of Coffin, under thermal cycle loading, turned out to be identical for a number of heat-resistant nickel-based alloys.

In this project tests were carried out under permanent visual surface observation and periodic photographing of the slip lines' orientation, the surface microcracks' initiation and the changes of the slip lines' orientation during thermal cycling with the optical magnification of 260 times. It should be noted that photographing during the course of the tests makes it possible to obtain high-quality images. TMF tests were conducted until failure or 2000 cycles, depending on which event happened first. After the tests the fracture surfaces were analyzed using optical fractography and a magnification of 160 times. Some tests were conducted on the samples with stress concentrators in the form of 0.5 mm holes.

2.3 Materials. The plates of the monocrystal alloy underwent the standard thermal treatment: heating in vacuum up to 1320 °C, holding at this temperature for 6 h, and cooling in argon. This was followed by double-stage aging in the mode: first stage, heating in air up to 1030 °C, holding at this temperature for 4 h; second stage, 24 h at 870 °C. The as-received crystal orientation is listed in **Table 1**.

Table1: Crystallographic orientation of single-crystal plates
Tabela 1: Kristalografska orientacija monokristalnih plošč

Number of the sample series	The crystallographic orientation of the samples along the longer axis	Deviation from exact orientation, degree	Azimuthal orientation, degree
1	[111]	5.64	8.26
2	[011]	4.51	11.27
3	[011]	8.33	14.43
4	[011]	9.67	7.86
5	[001]	5.47	41.97

3 RESULTS AND DISCUSSION

Despite the limited number of tests, the obtained experimental data allow us to formulate some

relationships which, of course, require further experimental verification.

3.1 Directions of the slip lines. The analysis of the test data shows that for different crystallographic orientations the slip lines form under different angles, including those oriented approximately across and along the loading vector, and also at an angle close to 45°. We obtained a reasonably good convergence between the experimentally measured and predicted slip lines. For a small number of cycles the nascent slip lines are oriented in the directions corresponding to the greatest Schmid factor. It should be noted that in the samples of series 3, 4 and 5 (**Table 2**) the slip lines corresponding to both, the octahedral and cubic slip systems, were observed (**Figure 3**), and in the samples of series 1 and 2, only those corresponding to the octahedral system were seen (**Figure 4**). Multiple slip and even patchy appears with an increase in the number of cycles. Microcracks initiate mainly on slip lines, but the direction of their growth does not depend on the direction of the slip lines, therefore, it has a non-crystallographic nature. Thus, initially, the microcrack is parallel to the slip lines, and then the crack turns out to be oriented along the sample axis (maximum compression). It is worth noting that no slip lines were found in this direction. Also, non-crystallographic directions of microcracks were observed in the micrographs of the fracture zones of all the samples (see **Figure 5**).

3.2 Orientation of the fracture surface

The character of the sample fracture can be seen in the scheme of **Figure 6** and the picture in **Figure 7**. The directions of the distribution of cracks were compared to the directions of the sliding lines.

The samples 3-0, 3-1, 3-3 of the series 3 [011] broke mainly in a zigzag line in the lattice plane, the samples 3-2, 3-4, 3-5 ruptured in the plane. At the upper edge of the section, the samples 3-0 and 3-5 were damaged by the rupture and the samples 3-1, 3-2, 3-3, 3-4 were damaged below the edge.

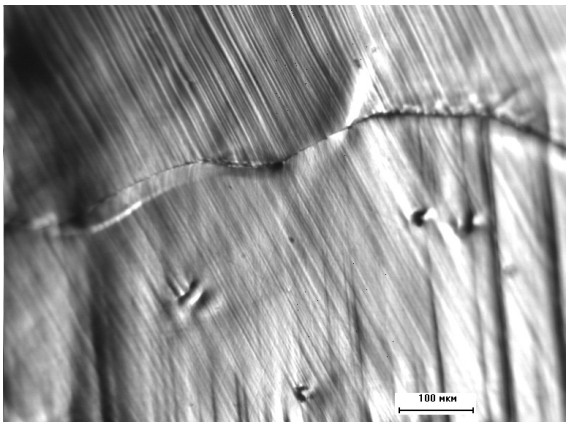

Figure 3: Microstructure of the surface of specimen 3-2 after 63 cycles (250–1000 °C)
Slika 3: Mikrostruktura površine preizkušanca 3-2 po 63 ciklih (250–1000 °C)

Table 2: Comparison of the calculated and experimental directions of the slip lines
Tabela 2: Primerjava izračunanih in eksperimentalnih smeri drsnih črt

Sample number	Exp. slip line slope [deg.]	Theor. slip line slope	
		octahedron	cubic
2-1	**10** 80; 82.5; 76.8; 78; 78.2; 82; 83; 84.2 93	**6.1** 81 95.8	- - -
2-2	**75.8; 80.5;88.8; 86** 99 114;126	81 - 95.8 -	- - - 132.8
2-4	**0; 1.3** 84.5	**0.2** 81	- -
2-6	**4.2; 3.8** 79.8; 81.2; 82; 85.8 93.5; 95.5	**6.1** 81 95.8	- - -
5-1	93.2	90.2	95.5
5-2	**3.5** 92.6 107.1	- 90.2 100.2	**5.3; 5.6** **95.5** -
5-3	**39.4** 90.6 149	**40.8** 90.2 150.2	- - -
1-6	**17.8** 131.2	**16.5** 130	- -
1-2	**22.4; 20.8** 130.5	**16.5** 130	- -
1-1	**15.8** 83.2; 82.5 128.5; 130.8	**16.5** 87.5 130	- - -
3-0	**15** 85 170.174	**-** 93.6 175.7	**14.8** -
3-1	**70.5** 89	**74.8** 93.6	
3-2	**35** 71.5 93.2	**-** 74.8 93.6	**38.6**
3-3	**91; 95.5** 169.2	**93.6** 167.5	
3-4	**21; 22.5** 65.5 93.2; 92.5; 92	**-** 74.8 93.6	**14.8**
4-1	**50** 78.5 155; 154; 162.4; 158.5	**48.8** 163.2	**-** 83.8; 84.9 -
4-2	**48.1; 51.2; 49.2; 48.5** 86.5; 81.5	**48.8** -	**-** **83.8; 84.9**

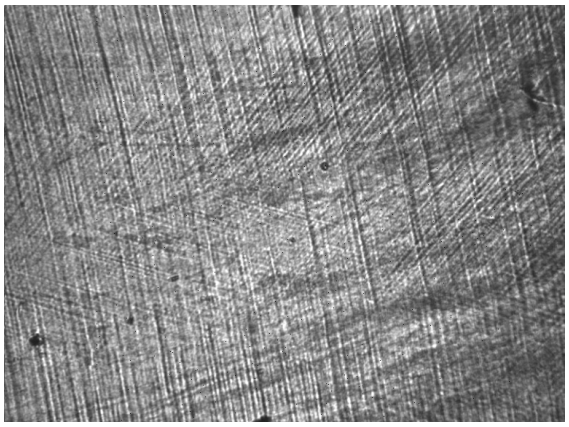

Figure 4: Microstructure of the fractured specimen 5-3
Slika 4: Mikrostruktura prelomljenega preizkušanca 5-3

Figure 5: Microstructure in the vicinity of the fracture of specimen 3-2
Slika 5: Mikrostruktura v bližini preloma vzorca 3-2

The samples of series 5 [001] broke perpendicularly to the loading vector along the lattice plane and at the angle toward the specimen plane (shear).

The samples 2-4 and 2-6, with concentrator of series 2 [011], broke perpendicularly to the loading vector along the plane and on the specimen plane. The sample 2-1 without a concentrator broke by shear in the plane and on the section.

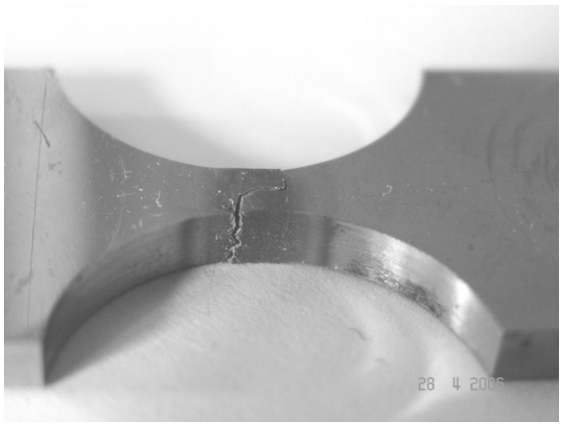

Figure 6: Appearance of the fractured specimen 3-0
Slika 6: Prelomljen preizkušanec 3-0

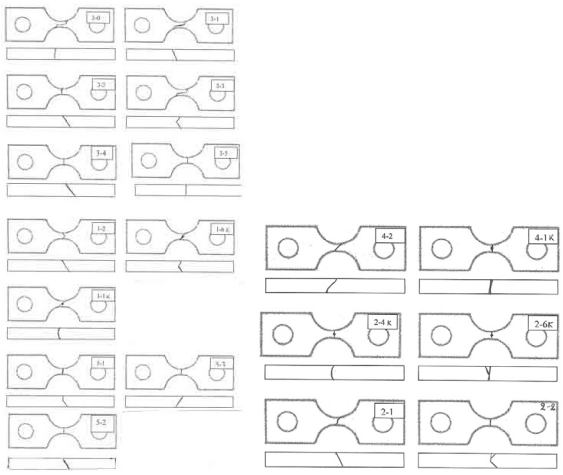

Figure 7: Course of the fracture lines in the specimens
Slika 7: Potek razpok v preizkušancih

The sample 4-1 of series 4 (with mixed orientation) with the concentrator was fractured perpendicularly to the loading vector, and the smooth sample 4-2 cracked at an angle toward the specimen axis and plane (shear).

The samples of series 1 [111] with and without a concentrator cracked by shear with a change of direction in the surface and in the section.

Table 3: Influence of the maximal temperature of a cycle on the number of total cycles to failure
Tabela 3: Vpliv najvišje temperature v ciklu na število ciklov do preloma

Sample number	Orientation	ΔT	T_{min}/°C	T_{max}/°C	N
3-0	011	750	150	900	951
3-1			200	950	450
3-2			250	1000	63
3-5		500	450	950	2535
3-3			500	1000	1220
3-4			550	1050	356
5-1	001	750	150	900	560
5-2			250	1000	95
2-4 with stress concentrator	011	500	350	850	2952
2-6 with stress concentrator			500	1000	187

3.3 Influence of the maximum temperature in the cycle

The data in **Table 3** show that the increase of the maximum temperature within the ranges 850–1000 °C and 900–1000 °C with the same total temperature amplitude decreases the service life to fracture by ≈15 times. If the maximal temperature is increased from 1000 °C up to 1050 °C with the same total temperature amplitude the time-to-fracture is decreased by approximately a factor of 4.

3.4 Influence of the total temperature amplitude

A decrease of the total temperature amplitude with a constant value of T_{MAX} = 1000 °C increases considerably the service life (**Table 4**).

Table 4: Influence of the temperature range on the number of cycles to fracture
Tabela 4: Vpliv razpona temperature v ciklu na število ciklov do preloma

Sample number	Orientation	T_{min}/°C	T_{max}/°C	*N*
3-2	011	250	1000	63
3-3	011	500	1000	1220
5-2	001	250	1000	95
5-3	001	500	1000	1460

3.5. Influence of the stress concentrator

Concentrators in samples in the form of holes with a diameter of 0.5 mm decrease the service life by ≈15 times (**Table 5**). At the same time, during the test of the sample with the concentrator and T_{max} = 850 °C a relatively large number of cycles before fracture (2952) was recorded. The sample without concentrator was not tested in such conditions, since the expected number of cycles before the fracture occurred was more than 10000.

Table 5: Influence of the stress concentrator on the number of cycles before destruction.
Tabela 5: Vpliv koncentratorja napetosti na število ciklov do preloma

Sample number	4-2	4-1 with stress concentrator	1-2	1-1 with stress concentrator	2-2	2-6 with stress concentrator
Orientation	[011]	[011]	[011]	[011]	[011]	[011]
T_{min}/°C	150	150	150	150	500	500
T_{max}/°C	900	900	900	900	1000	1000
N	308	25	823	50	472	187

3.6 Influence of the crystallographic orientation of material

The maximal thermal fatigue life in tests under the same thermal cycle modes was observed in the case of smooth samples with a [111] orientation and the minimal strength was obtained for the [011] direction (**Table 6**). Samples with a mixed orientation and [001] broke after a number of cycles decreasing in the series $N_{111} > N_{001} > N_{mix} > N_{011}$. At the same time, the notched samples with orientation [011] had a longer life than the samples with the orientation [111]. The reasons for such behavior require further research. The influence of the azimuthal orientation of single-crystal alloys [011] on the number of cycles before destruction is illustrated by the data in **Table 7**.

Table 6: Influence of orientation on the number of cycles before destruction.
Tabela 6: Vpliv orietacije na število ciklov do preloma

Sample number	Orientation	T_{min} /°C	T_{max}/°C	N
2-1	[011]	150	900	100
4-2	[011]			308
1-2	[111]			823
5-1	[001]			560
3-2	[011]	250	1000	63
5-2	[001]			95
2-2	[011]	500	1000	472
3-3	[011]			1220
5-3	[001]			1460
2-4 with stress concentrator	[011]	350	850	2952
1-6 with stress concentrator	[111]			320

Table 7: Influence of the azimuthal orientation of single-crystal alloys [011] on the number of cycles before destruction (T_{min} = 150 °C, T_{max} = 900 °C)
Tabela 7: Vpliv azimutne orientacije monokristala [011] na število ciklov do preloma (T_{min} = 150 °C, T_{max} = 900 °C)

Sample number	A deviation from exact orientation, degree	Azimuthal orientation, degree	*N*
2-1	4.51	11.27	100
3-0	8.33	14.43	951
4-2	9.67	7.86	308

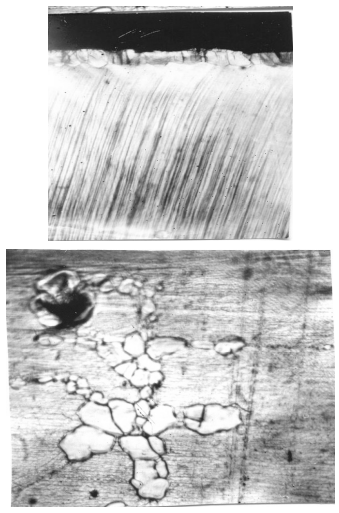

Figure 8: Microstructure of the surface of specimen 3-0 after 100 cycles (150–900 °C)
Slika 8. Mikrostruktura površine preizkušanca 3-0 po 100 ciklih (150–900 °C)

On of the samples the initiation of several microcracks, was observed often (but not always) oriented along the slip lines; some of the cracks originated near the pores. However, the fracture, as a rule, occurred from cracks located at some distance from the first microcrack.

3.7 Influence of the recrystallization

The recrystallization on sample 3-0 with the [011] crystallographic orientation hindered the development of slip lines. The microcrack initiation was observed on the sample surface beside the recrystallization areas (**Figure 8**). Nevertheless, these microcracks did not evolve into macrocracks and the sample fracture had a complex trajectory after a large number of cycles.

4 CONCLUSIONS

Within the framework of this project ingot blanks of single-crystal superalloys with five different crystallographic orientations were investigated. A new testing technique was developed, allowing obtain data on the role of the maximal and minimal cycle temperature, the stress concentration and the crystallographic orientation on the formation of slip lines, of microcracks and their propagation. On the basis of 18 tests with a maximum number of cycles equal to 2952 in the temperature range T_{min} = 150–500 °C, T_{max} = 850–1050 °C it was found that the thermal fatigue-crack initiation and growth are strongly influenced by the crystallographic orientation. Nevertheless, the fracture proceeds in a non-crystallographic mode and in some cases the cracks change their direction of propagation.

The following conclusions are proposed:

1. It was observed that the sample fracture takes place, depending on the orientation and the test mode, both in crystallographic and non-crystallographic directions independently of the crystallographic slipping.
2. Different directions of slip in different sections of the sample surface were discovered, including multiple slip.
3. A sharp reduction in fatigue life was observed with an increase in the maximum temperature in the cycle (with the same amplitude of temperature change).
4. The stress concentrators decrease significantly the fatigue life.
5. It was observed that the initial microcrack decelerates and stops and the sample fracture takes place on a newly nascent microcrack.

In the authors' opinion it would be useful to carry out further research, focusing on the detailed study of the fractured samples and thermal fatigue tests, keeping the samples at the maximum temperature for the same time interval in each cycle. Further study of the problem of the thermal fatigue strengths of the blades should concentrate on the development of computational methods for the deformation mode of single-crystal blades by creep and cyclic change of temperature, on the estimation of the blades' strength for thermal-cycle loading and on the development of a method for calculating the crack-growth rate, taking into account creep, stress concentration and fracture-mode changes.

Acknowledgement

The project was funded by the Pratt & whitney UTC Company. Special thanks are also due to Dr. Alexander Staroselsky, for problem formulation and program management.

5 REFERENCES

[1] P. A. S. Reed, X. D. Wu, Sinclair Fatigue crack path prediction in UDIMET 720 nickel-based alloy single crystals. Metallurgical and Materials. 31A (**2000**), 109–120

[2] J. Telesman , L. J. Ghosn. Fatigue crack growth behavior of a PWA 1484 single crystal superalloy at elevated temperatures. ASME Paper 95-GT-452, 1995

[3] K. S. Chan, J. Feiger, Y.-D. Lee, R. John, S. J. Hudak. Fatigue crack growth thresholds of deflected mixed-mode cracks in PWA1484, Journal of Engineering Materials and Technology. 127 (**2005**), 2–7

[4] S. X. Li, D. J. Smith, An overview of combined fatigue and creep response of single crystal nickel base superalloys. Proc. 5-th Liege Conf. on Materials for Advanced Power Engineering, Part II, October, 1974, Belgium, 1175–1184

[5] N. Marchal, S. Forest, L. Remy, S. Duvinage. Simulation of fatigue crack growth in single crystal superalloy using local approach to fracture. Euromech- mecamat 2006, Local approach to fracture, 9-12 May 2006

[6] A. I. Rybnikov, L. B. Getsov. New technique and results of thermal fatigue tests of superalloys and coatings. Proceedings of the sixth International Congress on Thermal Stresses. Vienna, Austria, 1 (**2005**), 305–309

[7] L. G. Padva, L. B. Getsov, O. S. Sadakov, A. I. Rybnikov Design method of strength estimation for gas turbine blades with coatings, Journal of Machinery Manufacture Under Reliability Problem, 4 (**1992**), 57–63

[8] Golubovskiy E., Svetlov I., Nozhnitsky Yu. Relationship of stress rupture and crystallographic orientation for Ni-base superalloys single crystal. EUCASS. European Conference for Aerospace Sciences. July 4-7, 2005, Moskow, Russia, CD

[9] Rtishchev V. V. Anisotropic alloys with columnar and single crystal structures used for blades of stationary gas turbine plants. Proc. 5th Liege Conf. on Materials for Advanced Power Engineering, Part II, October, 1994, Belgium, 1135–1144

[10] R. E. Shalin, I. L. Svetlov, E. B. Kachanov et al.: Single crystal nickel base superalloys, Mashinbuilding, (**1997**) 333 (In Russian)

[11] Erickson G. L., Harris K. Ds and sx superalloys for industrial gas turbines, Proc. 5th Liege Conf. on Materials for Advanced Power Engineering, Part II, October, 1994, Belgium, 1055–1074

[12] Jo C.-Y., Kim H.-M. Effect of recrystallisation on microstructural evolution and mechanical properties of single crystal nickel based superalloy CMSX-2 Part 2 – Creep behaviour of surface recrystallised single crystal., 19 (**2003**) 12, 1671–1676